Development of *Drosophila as* a metazoan model to study inorganic polyphosphate biology

Authors: Sunayana Sarkar[1], Harsha Sharma[1], Jayashree S Ladke[2], Sreejith Raran-Kurussi[1], Rashna Bhandari[2,#], Manish Jaiswal[1,#]

[1]Tata Institute of Fundamental Research Hyderabad, Ranga Reddy Dist. Hyderabad, 500046, India

[2]Centre for DNA Fingerprinting and Diagnostics, Inner Ring Road, Uppal, Hyderabad, 500039, India

[#]Corresponding authors: rashna@cdfd.org.in, manish@tifrh.res.in

Abstract:

Inorganic polyphosphate (polyP), a linear polymer of orthophosphate residues, is found in all living organisms. While the biological and molecular functions of polyP have been studied in prokaryotes and unicellular eukaryotes, in metazoans it has often been referred to as a molecular fossil. Although certain functions of polyP, e.g. in blood clotting, have been uncovered in humans, a genetically tractable model system has not been developed to systematically study polyP function in metazoans. To explore *Drosophila* as a model to study polyP, we first developed methods to quantify polyP in flies and then analysed polyP levels in various tissues during different developmental stages. Interestingly, we found that the levels of polyP increase before pupal formation and significantly drop during metamorphosis. To check the in-situ localization of polyP, we used polyP binding domain of bacterial protein, namely PPBD to detect endogenous polyP in fly tissues. We report the presence of polyP in cytoplasm and enrichment in the nucleolus in most tissue types. Interestingly, during oogenesis, we found polyP is enriched in early stage egg chambers but get depleted in later stages suggesting that polyP may play a crucial role during ovariole development. Finally, we found polyP to be enriched in fly hemocytes and showed that polyP promotes hemolymph clotting suggesting that polyP function between flies and mammals is conserved. These observations strongly suggest that combining powerful *Drosophila* genetic and biochemical tools can accelerate the discovery of unknown biological functions of polyP in metazoans.

Keywords: Polyphosphate, Polyphosphate staining, *Drosophila*, Hemocytes, Hemolymph Clotting, Developmental Regulation.

Introduction:

Inorganic polyphosphate (polyP) is a linear polymer of variable chain lengths of orthophosphate (Pi) residues linked via phosphoanhydride bonds. In the living system, polyP was first observed in bacteria *Spirillum volutans* and was named as volutin granules (Achbergerová and Nahálka, 2011; Wiame, 1947). Later, the presence of PolyP was reported in various species across evolution including mammals (Kornberg, 1995; Kornberg et al., 1999) However, due to the lack of understanding of its biological function in metazoans, polyP was often referred to as a molecular fossil. Recent strides in polyP biology in metazoans, however, have changed this paradigm. Excessive polyP accumulation in bacteria is believed to serve as a phosphate reservoir. In bacteria, polyP aids biofilm formation (Cremers et al., 2016) and mediates liquid-liquid phase separation (LLPS) (Wang et al., 2020). In algae, polyP buffers against alkaline stresses (Kornberg et al., 1999; Pick and Weiss, 1991). In mammals, the most well studied functions of polyP are in blood clotting (Cremers et al., 2016; Ghosh et al., 2013; Montilla et al., 2012; Omelon et al., 2009; Smith et al., 2010, 2006; Yoo et al., 2018) and bone mineralisation (Omelon et al., 2009). More recent studies have implicated PolyP in various biological phenomena in metazoans such as mitochondrial function (Seidlmayer et al., 2012) and neuronal activity (Bru et al., 2016b, 2017; Holmström et al., 2013). PolyP is also shown to act as an antioxidant (Archibald and Fridovich, 1982) and metal chelator (Dunn et al., 1994). Recently, polyphosphorylation of proteins on lysine residues, a novel post translational modification (PTM), has been identified (Azevedo et al., 2018, 2015), suggesting that polyP modifications of different proteins can affect a large number of biological processes that are yet to be uncovered.

Development of efficient tools for quantification and manipulation of polyP in prokaryotic models and yeast have been crucial to uncover various biological functions of polyP. Discovery of polyP synthases (PPKs in bacteria, and the VTC4 complex in yeasts)(Desfougères et al., 2020; Zhu et al., 2005) and polyphosphatases (PPXs and PPNs in bacteria and yeasts)(Alvarado et al., 2006; Bolesch and Keasling, 2000; Desfougères et al., 2020; Rangarajan et al., 2006; Ugochukwu et al., 2007; Wei et al., 2015; Zhu et

al., 2005), enzymes that synthesise and digest polyP respectively, were critical for genetic manipulation of polyP levels enabling phenotypic studies to probe biological functions. Recent work has reported that the Fo-F1 ATPase complex in the mitochondria is required for polyP synthesis in mammals (Baev et al., 2020). Purified human Prune protein was shown to have a short chain exopolyphosphatase activity in-vitro (Tammenkoski et al., 2008). Recently, biochemical experiments led to the discovery of endopolyphosphatase activity in the dinucleotide phosphatase NUDT3 (Samper-Martín et al., 2021). To date, only limited in-vivo studies on polyP biology in metazoans have been performed in *C.elegans*, guinea pig, and mouse models (Cremers et al., 2016; Ghosh et al., 2013; Nakamura et al., 2018; Omelon et al., 2009; Yoo et al., 2018). One of the major challenges in studying polyP in metazoans is the unavailability of a genetically tractable model system equipped with methods for visualisation, quantification and genetic manipulation of polyP. Development of tools to improve the visualisation of polyP in metazoan model organisms is thus crucial to understand the spatio-temporal regulation of polyP and their biological function.

Drosophila melanogaster, the fruit fly, has been a great model organism to study numerous biological processes. What makes flies unique among other models is the short life span, wealth of genetic mutants, and the availability of unparalleled tools for spatio-temporal genetic manipulations. In this work, we explored the idea of fruit fly as a model organism to study metazoan polyP biology. We developed and characterized simple methods to quantify polyP in fly tissues. Interestingly, we find polyP levels in flies are spatially and temporally regulated among different developmental stages and tissue types. We also show that polyP can promote hemolymph clotting in flies - a characteristic similar to that of blood clotting in mammals. This indicates that the molecular and biological functions of polyP between flies and humans is conserved and therefore studies of polyP using a fly model would facilitate the discovery of new functions of polyP in metazoans.

Results:

Standardisation of polyP extraction from *Drosophila*

Various biochemical strategies have been used to extract polyP from biological samples - a detailed comparison of those methods is described by Josep Clotet and his colleagues (Bru et al., 2016a). Acid based extraction fails to preserve the entire chain length of polyP as polyP is unstable in strong acids, whereas methods like column purification can only retain polyP of longer chain lengths (>60-80). PolyP extraction using saturated phenol in citrate buffer (pH=4.1), and chloroform followed by ethanol precipitation can efficiently pellet down polyP. This method, however, also allows co-purification of RNA, which may interfere with polyP quantification, depending on the quantification methods used. Therefore, to extract polyP from *Drosophila* samples, we sought to standardise the citrate saturated phenol-chloroform based method followed by RNase treatment. We lysed 10, 20, and 40 *Drosophila* larvae in the LETS buffer and subjected them to phenol-chloroform based extraction, which allowed separation of polyP and RNA in aqueous phase **(Fig 1a-b, Materials and Methods)**. We added RNaseA followed by a four hour incubation at 37℃. After another round of phenol:chloroform (1:1), the samples were subjected to ethanol precipitation to get rid of the RNase enzyme and residual nucleotides. The pellet was then dissolved in HPLC grade water. We divided the extracted samples into two equal halves and incubated one half with purified recombinant yeast exopolyphosphatase (*Sc*PPX) for 18 hours, at 37℃, to completely digest polyP **(Supplementary Fig 1, Materials and Methods)**. These samples were then used to quantify polyP following the method described below.

Standardisation of an enzymatic method for quantification of polyP from flies

A number of techniques based on Nuclear Magnetic Resonance (NMR), chromatography, radioactive isotope labelling, and enzymatic digestion have been used to quantify polyP. While most methods require a lot of samples, an enzymatic method of detection has been shown to be highly specific and may work with low polyP samples (Christ et al., 2020). Thus, to quantify the polyP extracted from fly tissues, we decided to standardise the enzymatic method. This method involved two steps - a) digestion of polyP

into monophosphates (Pi) using recombinant *Sc*PPX, and b) detection of Pi liberated after the digestion using Malachite Green (MG) (Van Veldhoven and Mannaerts, 1987). Malachite Green and Ammonium molybdate when mixed in the ratio 3:1 form a metachromatic brown coloured adduct that turns green upon conjugation with monophosphates (Hohenwallner and Wimmer, 1973; Petitou et al., 1978). This green compound absorbs maximally at 650 nm wavelength of light. Thus, with increasing Pi content in the solution, the intensity of the green colour increases **(Fig 1c)**. For calibration of the MG assay, increasing concentrations of KH_2PO_4 is used to draw a standard curve (Hohenwallner and Wimmer, 1973; Petitou et al., 1978). The absorbance measurements from digested polyP samples can be interpolated to quantify Pi released from extracted polyP samples. This allowed us to measure polyP content indirectly in Pi terms.

We recorded increasing amounts of polyP in accordance with an increasing number of larvae used for polyP extraction **(Fig 1d)**. We report each third instar larval polyP content as 565.5 +/- 326.2 picomoles in Pi terms **(Fig 1e)**. To normalise polyP content against total protein, we subjected larval lysates to protein quantification using Bradford assay before polyP extraction. The final polyP extracted in Pi terms was then normalised to the amount of protein. We recorded a polyP content of 46.8 +/- 6.8 picomoles Pi per mg protein from 10 effective third instar larval lysate **(Fig 1f)**. Normalised data sets are tabulated in **Fig 1g**. As the PolyP is extracted from whole larvae, this data does not account for tissue specific enrichment of polyP.

Polyphosphate levels are developmentally regulated

Drosophila life cycle involves embryonic, larval, pupal and adult stages. To test if polyP levels are developmentally regulated, we quantified polyP levels from embryonic to adult (pharate) stages. First, we collected embryos at every two-hour interval from egg laying till 18 hours. We extracted polyP at every two-hour intervals of embryonic development and quantified polyP from 50-75 embryos in each set using MG assay. As shown in **Fig 2a**, we did not observe any obvious change in polyP levels across

various embryonic stages. We then compared polyP levels between various life cycle stages. We estimated polyP content from embryos (75 embryos, 0-18 hours, in each set), four different larval stages (first instar, 25 in each set; second instar, 25 in each set; feeding third instar, 10 in each set; and non-feeding third instar, 10 in each set), two pupal stages (prepupae, 20 in each set collected within a period of two hours and one day old pupa, 20 in each set), and adult (pharate, 10 in each set) stage. We found that polyP content remains unchanged from embryos to third instar feeding crawling larval stages. Interestingly, we recorded a significant increase in polyP content in the third instar non-feeding wandering larval stage (stage used for polyP quantification in **Fig 1**). We further noted that polyP content reduces during the prepupal stage and remains unchanged until late pupal stage. We again recorded a significant drop in polyP levels in the adult (pharate) stage **(Fig 2b)**. This data suggests that polyP, which is accumulated at the late third instar larval stages, perhaps acts as a phosphate reservoir to be used for metamorphosis during the pupal stage.

Polyphosphates are enriched in post lysosomal fraction

In mammalian cells polyP has been found in various subcellular compartments, such as vacuoles, mitochondria, and nucleus, even in lysosomes. On the other hand, in yeasts, polyP is found specifically in vacuoles indicating that polyP localization and functions in eukaryotes may have evolved between yeasts and mammals. Thus we sought to investigate the relative levels of polyP in various subcellular compartments of fly larvae. We extracted and quantified polyP from nuclear, mitochondria, lysosome enriched, post lysosomal and cytosolic fractions from larval extracts (20 in each set) using MG assay. We observed that although polyP is present in considerable amounts in nucleus, mitochondria, and lysosome enriched fractions, most of the polyP is present in the post lysosomal fraction. This post lysosomal fraction consists of small vesicles, and organelles, which can also be sites of polyP storage **(Fig 2c)**. This data suggests that subcellular distribution of polyP in larvae is similar to that of mammals. Moreover, the spatial distribution of polyP across cells and tissues can be determined better by in-situ labelling of polyP.

In-situ labelling of polyP in *Drosophila* tissues

We sought to characterise in-situ labelling of polyP in fly tissues. To detect polyP we used bacterial protein previously reported to bind polyP. Polyphosphate Binding Domain from *E.coli* exopolyphosphatase (PPBD) has been shown to bind polyP in vitro, as well as in yeast and human cells (Saito et al., 2005). We prepared a GST tagged recombinant PPBD (GST-PPBD) construct and purified this recombinant GST-PPBD protein to label polyP in fly tissues. We used purified GST protein as a negative control to detect any non-specific interaction. *Drosophila* tissues were dissected and fixed with 4% paraformaldehyde. Fixed tissues were permeabilized and divided into two parts- one part was incubated with GST-PPBD, and the other with GST (control) followed by detection using anti-GST antibodies and fluorophore labelled secondary antibodies **(Fig 3a, Materials and Methods)**.

We found GST-PPBD labelling in a punctate pattern in the cytoplasm, and inside nuclear compartments **(Fig 3b)**. In cells with larger nuclei, e.g in salivary glands, GST-PPBD labelling is clearly visible in these subnuclear compartments devoid of nuclear DAPI staining **(Fig 3b ii,iv)**. We suspected these compartments to be nucleolus. To test this possibility, we co-stained GST-PPBD with Fibrillarin, a nucleolar protein, and found colocalization of these proteins suggesting that polyP is enriched in nucleolus **(Fig 3c-d)**. This nucleolar polyP presence is particularly interesting, as it resembles the finding of polyP in nucleolus of HeLa cells by Paul A.Wender and his colleagues, and also suggests a role of polyP storage and/or function in these phase separated moieties (Beaufay et al., 2021; Fernandes-Cunha et al., 2018; Wang et al., 2020). We systematically tested many larval imaginal discs (tissues that would mature into organs of the adult fly), and found a similar pattern of punctate cytoplasmic and nucleolar GST-PPBD staining in most of them, e.g, wing discs **(Fig 3e-g)**. We could not detect considerable nuclear signals from leg imaginal discs, and tissues like haltere imaginal discs showed no difference in GST-PPBD staining when compared to the GST control **(Supplementary Fig 2 e-h)**. The primary lobe of lymph gland also showed a clear nuclear associated punctate GST-PPBD staining when compared to GST control **(Supplementary Fig 2o-p)**. Interestingly, GST-PPBD labelling revealed spatial and temporal dynamics of polyP localization during oogenesis. We observed intense GST-PPBD staining

inside the nuclear compartments and also in the cytoplasm of the nurse and follicle cells in early stages of ovary development **(Fig 4b)** as compared to the GST control **(Fig 4a)**. Intriguingly, during oogenesis we noted a gradual reduction in the intensity of GST-PPBD staining from S2 to S9 egg chambers indicating a gradual reduction in polyP levels **(Fig 4b).** This observation suggests that the developmental regulation of polyP levels may have a crucial role during oogenesis. Overall, this is a first comprehensive tissue staining report exhibiting the spatio-temporal dynamics of polyP within an organism.

PolyP is enriched in hemocytes

During the in-situ labelling of polyP with GST-PPBD, we found granular punctate nuclear associated signals from lymph glands **(Supplementary Fig 2o-p)**. Thus, we sought to test the possibility of conserved polyP functions between flies and mammals. One of the most well studied functions of polyP in mammals is that of blood clotting. PolyP was found to be enriched in human platelets in the form of dense granules (Ruiz et al., 2004) and it has been shown to be released from activated platelets to promote blood clotting (Smith et al., 2010, 2006). Crystal cells, a type of hemocyte in *Drosophila* hemolymph, are known to be similar to platelets (Vlisidou and Wood, 2015). Crystal cells and plasmocytes, another type of hemocytes, are known to be crucial for hemolymph clotting in flies (Vlisidou and Wood, 2015). Both these cell types differentiate from their progenitors in the larval lymph glands (Grigorian et al., 2011). To stain mature hemocytes from hemolymph, we bled 10 larvae and let the hemocytes adhere to cover slips followed by GST-PPBD staining **(Method adopted from (Handke et al., 2013), See Materials and Methods)**. Plasmocytes and Crystal cells were identified based on the cell specific marker lines - *hml-Gal4>UAS-GFP* (Sinenko and Mathey-Prevot, 2004) and *lz-Gal4>UAS mCD8-GFP* (Sinenko et al., 2004) respectively. We found an intense granular GST-PPBD labelling both in plasmocytes and crystal cells as compared to GST control **(Fig 5a-d)**. These results revealed the similarity of granular polyP expression in fly hemocytes and mammalian platelets.

PolyP promotes hemolymph clotting in flies - an evolutionarily conserved function

PolyP, upon release from platelets, acts as a proinflammatory and procoagulant mediator (Müller et al., 2009; Smith et al., 2006), activates blood clotting factors (Montilla et al. 2012; Weitz and Fredenburgh 2017; Smith et al. 2006; Suess et al. 2020; Smith et al. 2010; Morrissey and Smith 2015), and gets integrated within the fibrin clots in mammals (Ghosh et al. 2013). The thickness and density of the fibrin clot fibre increases upon increasing the concentration and length of polyP (Ghosh et al., 2013; Smith et al., 2010, 2006). *Drosophila* hemolymph also undergoes clotting and some of the hemolymph clotting factors are conserved between flies and human (Dziedziech et al. 2019; Bidla et al. 2005; Scherfer et al. 2004; Karlsson et al. 2004). To find, if the function of polyP is conserved between flies and mammals, we tested the effect of addition of polyP in hemolymph clotting ex-vivo. We collected 4ul hemolymph from effective 12 third instar larvae and incubated with either polyP (1.6 nmol polyP in Pi terms, equivalent to the total polyP content from two larvae) or Pi (1.6 nmol Pi) or water, followed by incubation at 25℃ in a humid chamber for 30 minutes to allow clotting. Interestingly, we found significantly increased thickness of clot fibres upon incubation of hemolymph with polyP (P_{14}, P_{65}, P_{130}) as compared to when only water or Pi was added to the hemolymph **(Fig 5e-m)**. Further, addition of medium and long chain polyP (P_{65}, P_{130}) resulted in a significant increase in the number of fibres formed at the circumference of the clotting hemolymph drop as compared to the addition of water or Pi or short chain polyP (P_{14}) **(Fig 5n-v, Supplementary Fig 3**). This shows that polyP increases both the number and thickness of clot fibres during hemolymph clotting. Overall, these results suggest that polyP function in hemolymph/blood clotting is conserved between flies and humans.

Discussion:

In this work, we report methods to extract, quantify and visualise polyP in *Drosophila*. We employed these methods to check polyP levels in various developmental stages and tissues and found that polyP in *Drosophila* is spatially, temporally, and developmentally regulated. Importantly, we report that polyP accumulated in granular forms in hemocytes and it can accelerate hemolymph clotting. These data suggest that polyP function is conserved across evolution and *Drosophila* can serve as a metazoan model

to probe for polyP functions.

Biochemical estimation of polyP

We standardised citrate saturated phenol and chloroform based methods to extract polyP as it allows purification of all chain lengths (Bru et al., 2016a; Christ et al., 2020), however, with the caveat of copurification of RNA. Therefore, we decided to incorporate an additional RNase treatment step to our extraction protocol. We also determined that a complete digestion of polyP from extracts requires ~18 hours of 37°C incubation with the recombinant *Sc*PPX purified in our lab. These characterisations were necessary since RNA in extracted polyP have been shown to interfere with polyP quantification (Bru et al., 2016a), and also, an incomplete digestion of polyP will result in underestimation of polyP content. We for the first time report an account of biochemical detection of polyP from flies and reveal its quantity. To quantify polyP, due to high specificity we employed the method of enzymatic degradation of polyP into Pi and measurement of Pi released using MG **(Fig 1b)**. We categorically exploited the sensitivity of our assay and found that polyP pellets from maximum 20 larvae dissolved in 50ul (undiluted) could be assayed by MG without saturating the signals. We thus chose 10 larvae to be a suitable average number of larvae used in experiments to assay polyP content **(Fig 1e,f).** Commercially available Phosfinity kits can detect phosphate content of polyP (Phosfinity Quant) efficiently, provided the concentration of liberated Pi is in micromolar range. On the other hand, we report *Drosophila* larvae to have low picomolar levels of Pi liberated on *Sc*PPX treatment of polyP. Thus we could not use the Phosfinity Quant kit, and instead standardised MG assay for quantification.

Tissue staining for in-situ detection of polyP

Fluorescent dyes DAPI and JCD7/JCD8 have been used to stain polyP in cells (Angelova et al., 2014; Arredondo et al., 2022; Kulakova et al., 2011). JCD7 and JCD8 are reported to detect polyP, however, it is highly expensive at the moment. DAPI, the most widely used dye when excited at 405 nm gives a specific polyP fluorescence signal at 550 nm (Aschar-Sobbi et al., 2008; Kulakova et al., 2011; Omelon

et al., 2016; Tanious et al., 1992). This spectral property has been exploited, even with its following limitation- DAPI-RNA fluorescence maxima is at 525 nm. We, however, could not get consistent staining of polyP with DAPI in all tissues. Possibly due to the very low content of polyP in flies, this method was not as sensitive as it is in other biological systems. We then tried staining polyP using the polyP binding domain of *E.coli* exopolyphosphatase - PPBD. Detection of polyP by PPBD has been used earlier in cells. (Saito et al., 2005). We report a comprehensive account of tissue staining of polyP using PPBD in fly tissues **(Fig 3,4 Supplementary Fig 2)**.

Together, biochemical detection of polyP from various fly life cycle stages and in-situ localization studies in various tissues revealed that polyP levels are spatially and temporally regulated. It was interesting to observe that polyP levels increase in late larval stages, just before the pupariation **(Fig 2b)**. PolyP levels, however, gradually decrease during metamorphosis. We hypothesise that phosphates are stored during the late larval stage in the form of polyP, which then is used as a phosphate reservoir during metamorphosis, which is essentially a non feeding stage of the fly life cycle. Similarly, GST-PPBD staining revealed a developmental regulation and localisation of polyP in developing ovaries **(Fig 4)** - polyP levels are gradually decreased during the development of egg. These results suggest that polyP may play a crucial role during the development of an organism.

PolyP function is evolutionarily conserved

Role of polyP in blood clotting is one of the most well studied functions of polyP in mammals (Ghosh et al., 2013; Montilla et al., 2012; Morrissey and Smith, 2015; Müller et al., 2009; Puy et al., 2016; Ruiz et al., 2004; Smith et al., 2012, 2010, 2006; Suess et al., 2020).These studies are primarily based on the fact that polyP is intensely expressed in and released from platelets, and addition of polyP to plasma can accelerate clotting with increased clot fibre density and thickness. We show an abundant polyP labelling in hemocytes **(Fig 5a-d)**, and report addition of polyP can promote hemolymph clotting **(Fig 5e-v)**. This strongly suggests the role(s) of polyP in blood clotting in mammals and hemolymph clotting in flies is

conserved. Most of the studies on polyP mediated blood clotting are done in an ex-vivo system due to limitation of genetic manipulations. Generation of a fly model can accelerate the discoveries of such fundamental polyP functions. Studies in flies can also shed light on the regulation, release and function of polyP in hemocytes. Therefore, systematic analysis of polyP in flies will provide novel insight to various biological and molecular functions of polyP in metazoans.

Further studies of polyP function will require unbiased phenotypic analysis when polyP are depleted from fly tissues in spatial and temporal manner. As the machinery for polyP synthesis and depletion in flies is not known, genetic manipulation of polyP is not feasible. Therefore, we are developing transgenic lines to express yeast exopolyphosphatase (*Sc*PPX) in flies to deplete polyP spatially and temporally. Further, genetically encoded sensors will be required for studies of precise regulation of polyP dynamics in vivo - generation of such fluorescence based sensors may facilitate screens to identify the genes required for polyP regulation.

Materials and methods:

Polyphosphate extraction:

Fly tissues were lysed in the LETS buffer. For 20 third instar larvae, a 200ul buffer was used. To precipitate the genomic DNA, we added acid phenol (pH=4.5), equivalent to the volume of the buffer and centrifuged at 18000g for 10 minutes at room temperature. The aqueous phase, which is devoid of the genomic DNA, was transferred in a fresh vial and mixed with double volume of chloroform. The mixture was vortexed for three minutes and centrifuged at 18000g for five minutes at room temperature. The aqueous phase devoid of proteins were collected and divided into two halves. One half was treated with RNase, and the other left untreated. Both tubes were incubated at 37℃ for four hours before addition of 1:1 phenol:chloroform mixture equivalent in volume of the sample to them. The solutions were vortexed for three minutes and centrifuged at 18000g for five minutes at room temperature, The aqueous phase devoid of RNase enzyme and RNA remnants were collected and chloroform was added to them in a volume double that of the samples. The mixture was vortexed for three minutes and

centrifuged at 18000g for five minutes at room temperature. The aqueous phase was collected and mixed with absolute ethanol in the ratio (vol:vol) 1:2.5, followed by overnight incubation at -80℃. Next day, the polyP was precipitated by a 30 minute centrifugation at 18000g at 4℃. Ethanol was decanted and the transparent polyP pellet was dissolved in water.

LETS buffer: Lithium Chloride (100 mM), EDTA (10 mM), Tris-Cl pH=8 (10 mM), SDS (0.2%).

Polyphosphate quantification using Malachite Green Assay:

Malachite Green detects monophosphates released from polyP pools due to addition of purified yeast exopolyphosphatase (*Sc*PPX). Samples with extracted polyP were divided into two parts and one part was treated with 5ug/ml of *Sc*PPX for 18 hours at 37℃ while the other half acted as the untreated control. Malachite Green reagent was prepared by mixing Malachite Green and Ammonium molybdate in 3:1 ratio. For phosphate standards, we used K_2HPO_4. We loaded a 50 ul of sample mixture and standards into 96 well plates and 200 ul of MG reagent followed by a 15 minute room temperature incubation in dark. The absorbance measurements were taken in Omega Polar Star Plate Reader at 650 nm. From the standard curve, interpolation was done to figure out polyP content of samples (in Pi terms)

Cell fractionation:

30 third instar larvae were collected and washed with 1X TBS and water before adding to ice cold mitochondrial isolation buffer and crushing on ice. To get rid of debris, the lysate was centrifuged at 200 rcf for five minutes. The supernatant was carefully collected and nuclear fragment precipitation was done by centrifuging the sample at 1500 rcf for 8 minutes, the supernatant is collected and centrifuged at 8000 rcf for 15 minutes to pellet down mitochondrial fragment. The supernatant was collected and separated. The mitochondrial pellet was dissolved in a fresh ice cold mitochondrial isolation buffer and centrifuged at 8000 rcf for 15 minutes to wash the pelleted down mitochondrial fragment, The supernatant is collected separately and centrifuged at 20000 rcf for two hours to pellet down lysosomes. The supernatant containing the rest of cytoplasmic organelles were centrifuged at 150000 rcf for 1.5

hours to pellet down all other organelles and vesicles and granules and have a clear cytosol as supernatant. All the pellets were resuspended in mitochondrial isolation buffer and polyP extraction was then carried out with all the fragments collected following **Polyphosphate extraction** procedure mentioned above.

Mitochondrial Isolation buffer: Mannitol (210 mM), Sucrose (70 mM), EGTA (1 mM), HEPES pH=7 (5 mM), BSA (0.5%)

Embryo collection:

Flies acclimatised on the grape juice plates for 24 hours were used for egg laying for two hours on a fresh grape juice plate. Every two hours AEL, we collected the embryos for polyP extraction. The eggs were incubated at 25℃ for 18 hours. We used 150 embryos for each set in our experiment.

GST-PPBD staining

Tissues were dissected in 1X TBS, and fixed in 4% paraformaldehyde for 20 minutes. They were then subjected to three 1X TBST (0.2% Triton X-100) washes, 10 minutes each. 5% NGS (nascent goat serum) was added to the tissues as a blocking agent, and incubated for one hour at room temperature. The tissues were next incubated with 25ng/ul GST or GST-PPBD (purification process mentioned in GST and GST-PPBD Protein Purification section of methods) for one hour at room temperature followed by three 1X TBST washes, 10 minutes each. The tissues were then incubated in mouse anti-GST antibodies overnight at 4℃. Next day, the tissues were washed thrice with 1X TBST and incubated with goat anti mouse antibodies at room temperature for two hours. Following incubation, the tissues were washed thrice with 1X TBST and incubated with 100uM DAPI to stain nuclei for 15 minutes at room temperature. DAPI staining was followed by a final step of three washes with 1X TBST before mounting the dissected tissues on slides for imaging. Images were acquired with Leica STELLARIS 5 confocal microscope with 63X oil objective lens (HC PL APO 63x/1.40 OIL CS2)

Protein Purification:

***Sc*PPX purification**

Transformed BL21(DE3) competent cells with 100 ng of pTrcHis PPX were taken and incubated as primary culture in 100 ml 100 ug/ml ampicillin containing LB overnight at 37℃. The OD_{600} is checked and diluted 1 Litre LB media and incubated at 37℃ till OD_{600} reaches 0.8. The culture was induced with 1 mM IPTG for 4-6 hrs at 30℃ and 180 rpm. The cells were pelleted by centrifugation at 3000 rcf for 15 min at 4℃. We can at this point discard the supernatant and store the induced pellet in -80℃ for an indefinite period. The pellet was resuspended in a 12 ml ice cold lysis buffer. This was followed by lysis of the cells by sonication (2 min, output voltage 20, output control 30, duty cycle 30/40) on ice till the lysate becomes clear.We harvested lysate by centrifugation at 15000 rcf for 20 min at 4℃. Next the supernatant is transferred to an equilibrated Ni-NTA column and incubated in the rotor at 4℃ for 2 hours. The protein is subjected to affinity chromatographic purification under gravity. The flow through was collected from the column under gravity at room temp. The column was then washed with Wash buffer I, wash buffer II, and eluted in elution buffer. The protein collected was subjected to size exclusion chromatography and run on Sephadex-200 sizing column to elute isolated fractions of *Sc*PPX protein. The protein was divided into single use aliquots and stores in -80℃.

Lysis buffer: NaCl (100 mM), Tris pH=8.0 (25 mM)

Wash buffer I: NaCl (100 mM), Tris pH=8.0 (25 mM), Imidazole (50 mM)

Wash buffer II: NaCl (100 mM), Tris pH=7.4 (25 mM), Imidazole (75 mM)

Elution buffer: NaCl (100 mM), Tris pH=7.4 (25 mM), Imidazole (100-300 mM)

GST and GST-PPBD Protein Purification

Transformed BL21(DE3) competent cells with 100 ng of pGEX-6P2-GST and pGEX-6P2-GST-PPBD respectively were taken and incubated as primary culture in 100 ml 100 ug/ml ampicillin containing LB overnight at 37℃. The OD_{600} is checked and diluted in 500ml LB media and incubated at 37℃ till OD_{600} reaches 0.8. The culture was induced with 1 mM IPTG for 4 hrs at 37℃ and 180 rpm. The cells were

pelleted by centrifugation at 3000 rcf for five min at 4℃. Pellet was resuspended in 50 ml bufferA and lysed by sonication (2 min, output voltage 20, output control 30, duty cycle 30/40). We harvested lysate by centrifugation at 14000 rcf for 10 min at 4℃ and added TritonX100 to a final concentration of 0.1%. For equilibration, 250ul glutathione beads slurry was washed with twice the volume of buffer B and beads were settled by centrifugation at 400g for three minutes at 4℃. The beads resuspended in 1:1 buffer B were transferred to the cell lysate. The lysate was mixed at 4℃ for 2.5 hours, and next day, beads were pelleted at 400g for three minutes at 4℃. The beads were washed thrice with buffer C with centrifugation at 400g for three minutes at 4℃ at each step, and again thrice with buffer B with centrifugation at 400g for three minutes at 4℃ at each step, followed by two washes with PBS with centrifugation at 400g for three minutes at 4°C at each step. This was next washed with 1 ml 50mM Tris pH=8 twice with centrifugation at 400g for two minutes at 4℃ at each step. This was then mixed with 200ul glutathione and incubated overnight on a rotor at 4℃. The mix is centrifuged for three minutes at 400g at 4℃ and the supernatant is carefully removed. The supernatant is the protein required.

Buffer A: HEPES pH=6.8 (20mM), NaCl (100mM), EDTA (2mM), DTT freshly added (5 mM)

Buffer B: Buffer A, TritonX100 (1%)

Buffer C: HEPES pH=6.8 (20mM), NaCl (500mM), EDTA (2mM), TritonX100 (1%)

Elution buffer (1ml): TrispH=8 (50mM), Glutathione (50mM), 12 ul of 1M NaOH

Hemocyte adherence and assessment of clot fibre thickness and numbers

For adherence, the hemolymph was collected from 10 larvae in 15ul TBS and allowed to adhere on coverslip at room temperature for 30 minutes, a method adopted from (Handke et al., 2013) . The supernatant was taken out carefully and the adhered cells were fixed using 4% PFA for 20 minutes. This was followed by immunostaining with GST-PPBD using the GST-PPBD staining procedure mentioned above. For thickness measurements, 25 larvae were collected, washed in 1X TBS and dried on tissue paper. The dorsal side abdominal region was gently teared to let only hemolymph ooze out. The hemolymph was then collected and divided into sets of two 4ul drops. These 4ul hemolymph (equivalent

to 12 larvae) was mixed with either 2ul water and 2ul Pi (1.6 nmole, equivalent to the content of 2 larval polyP) or with 2ul water and 2ul PolyP (P_{14},P_{65},P_{130}) each containing 1.6 nmole Pi terms already added on a slide. The slide was inverted and the hanging drop was incubated at 25°C in a humid chamber for 30 minutes. Post incubation, cover slip was placed on the drop and clot fibres were imaged using Olympus BX53 upright microscope with 40X oil objective lens (40x/NA 1.40/Oil UPLX APO) fitted with Retiga-R6 camera. Post imaging, the thickness of the fibres were measured by drawing lines across the mid fibre length using ImageJ software. For assessment of the the number of clot fibres, 1ul water and 1ul Pi (0.8 nmole) and 1ul PolyP (P_{14},P_{65},P_{130}) each containing 0.8 nmole Pi terms) were added on the slide as drops, and 2ul hemolymph was mixed. The slide was incubated at room temperature (24°C) for 20 minutes to allow evaporation. Post incubation, clot fibres were imaged using Olympus BX53 upright microscope with 40X oil objective lens (40x/NA 1.40/Oil UPLX APO) fitted with Retiga-R6 camera. Post imaging, the number of fibres were measured by manual counting.

Graph and statistical analysis:

All the graphs and statistical analysis were done using Graphpad Prism software.

Fly lines:

Name	**Flybase ID**	**References**
Canton-S	FBsn0000274	
Hml-Gal4 > UAS-GFP	FBst0030140	(Sinenko and Mathey-Prevot, 2004)
Lz-Gal4 > UAS-mCD8-GFP	FBst0006314	(Sinenko et al., 2004)

Material:

#	**Name**	**Company**	**Catalogue ID**
1	100% molecular grade ethanol (diluent for DNA extraction)	Himedia	MB228

2	4% paraformaldehyde	Himedia	TCL119
3	Acid phenol	Himedia	MB081
4	Ammonium Molybdate	Himedia	GRM307
5	BL21 DE3 competent cells	Himedia	MBT143
6	Boric acid	Himedia	MB007
7	Bovine Serum Albumin	Himedia	MB083
8	Chloroform	Himedia	MB019
9	D-Mannitol	Himedia	MB198
10	DAPI hydrochloride	Himedia	MB097
11	DL-DTT	Himedia	MB070
12	EDTA	Himedia	GRM1370
13	EGTA	Himedia	MB130
14	Goat anti-mouse-alexa555	Invitrogen	A32727
15	Goat anti-rabbit-alexa-488	Invitrogen	A11034
16	HEPES	Himedia	MB016
17	HPLC grade water	Himedia	AS077
18	Imidazole	Himedia	MB019
19	L glutathione reduced	Sigma	G4251
20	Lauryl sulphate (SDS)	Himedia	MB010
21	Lithium chloride	Himedia	MB038
22	Luria Broth	Himedia	M575
23	Luria Broth Agar	Himedia	M1151
24	Malachite Green	Glentham Life Sciences	GD8088
25	Mouse anti-GST	Cell Signaling Technology	2624
26	Ni-NTA agarose	Qiagen	30210

27	P_{14}, P_{65}, P_{130} (Ex-polyP set)	Regenetiss	Gifted by T.Shiba
28	Pierce glutathione agarose	Thermo scientific	16100
29	Potassium phosphate dibasic anhydrous	Himedia	MB044
30	Rabbit Anti-Fibrillarin	CST	2639
31	RNase A	Himedia	DS0003
32	Sodium chloride	Himedia	MB023
33	Sodium hydroxide	Himedia	MB095
34	Sucrose	Himedia	MB025
35	Tris free base	Himedia	MB029
36	Triton X100	Himedia	MB031

Serial number	**Plasmid name**	**Source**
1	pTrcHisPPX	This work
2	pGEX-6P2-GST-PPBD	This work
3	pGEX-6P2-GST	This work

Acknowledgements

We thank T. Shiba for sharing polyP of different chain lengths -polyP (P_{14}, P_{65}, P_{130}). We also thank Shubham Kumar Agrawal for help with purification of *Sc*PPX and Manisha Mallick for assistance with polyP analysis by gel electrophoresis. We thank Dr. Lolitika Mandal for sharing fly lines with us. We thank Dr. Aprotim Mazumder for sharing antibodies. We thank Dr. Vipin Agarwal for sharing the SEC setup for protein purification. We forward our gratitude to Dr. Jim Morrisey for his expert comments during the very initial stages of the project. We thank Dr. Henning Jacob Jessen, Dr. Anand T Vaidya, Dr. Kalyaneswar Mandal, Dr. Vinay Bulusu and Dr. Sonal Nagarkar Jaiswal and members of the Laboratory of Cell Signalling, CDFD and Fly lab, TIFRH for discussions and valuable feedback.

Funding

This work is funded by DBT-DFG grant IC12025(11)/2/2020-ICD-DBT to MJ and RB. MJ is supported by the Department of Atomic Energy (Project Identification No. RTI4007), Department of Science and Technology, SERB (CRG/2020/003275), Department of Biotechnology (BT/PR32873/BRB/10/1850/2020), Government of India. MJ is a Ramalingaswami fellow, Department of Biotechnology, Government of India, underproject number BT/RLF/Re-entry/06/2016. R.B. acknowledges support from the Department of Biotechnology, Ministry of Science and Technology, Govt. of India. (BT/PR29960/BRB/10/1762/2019); Science and Engineering Research Board, Department of Science and Technology, Govt. of India (CRG/2019/002597); and CDFD core funds. JSL is supported by a Shyama Prasad Mukherjee Fellowship from the Council of Scientific and Industrial Research, Government of India.

Author contributions

SS, RB and MJ have conceptualised the study. SS: Designed and performed most experiments and analysed the data. HS: GST-PPBD labelling. JSL: Analysis of polyphosphate by gel electrophoresis. SRK: Size Exclusion Chromatography for *Sc*PPX purification. SS, RB and MJ: Wrote the manuscript.

Everyone has read and edited the manuscript.

References

1. Achbergerová L, Nahálka J. 2011. Polyphosphate--an ancient energy source and active metabolic regulator. *Microb Cell Fact* **10**:63. doi:10.1186/1475-2859-10-63
2. Alvarado J, Ghosh A, Janovitz T, Jauregui A, Hasson MS, Sanders DA. 2006. Origin of exopolyphosphatase processivity: Fusion of an ASKHA phosphotransferase and a cyclic nucleotide phosphodiesterase homolog. *Structure* **14**:1263–1272. doi:10.1016/j.str.2006.06.009
3. Angelova PR, Agrawalla BK, Elustondo PA, Gordon J, Shiba T, Abramov AY, Chang Y-T, Pavlov EV. 2014. In situ investigation of mammalian inorganic polyphosphate localization using novel selective fluorescent probes JC-D7 and JC-D8. *ACS Chem Biol* **9**:2101–2110. doi:10.1021/cb5000696
4. Archibald FS, Fridovich I. 1982. Investigations of the state of the manganese in Lactobacillus plantarum. *Arch Biochem Biophys* **215**:589–596. doi:10.1016/0003-9861(82)90120-5
5. Arredondo C, Cefaliello C, Dyrda A, Jury N, Martinez P, Díaz I, Amaro A, Tran H, Morales D, Pertusa M, Stoica L, Fritz E, Corvalán D, Abarzúa S, Méndez-Ruette M, Fernández P, Rojas F, Kumar MS, Aguilar R, Almeida S, van Zundert B. 2022. Excessive release of inorganic polyphosphate by ALS/FTD astrocytes causes non-cell-autonomous toxicity to motoneurons. *Neuron* **110**:1656-1670.e12. doi:10.1016/j.neuron.2022.02.010
6. Aschar-Sobbi R, Abramov AY, Diao C, Kargacin ME, Kargacin GJ, French RJ, Pavlov E. 2008. High sensitivity, quantitative measurements of polyphosphate using a new DAPI-based approach. *J Fluoresc* **18**:859–866. doi:10.1007/s10895-008-0315-4
7. Azevedo C, Livermore T, Saiardi A. 2015. Protein polyphosphorylation of lysine residues by inorganic polyphosphate. *Mol Cell* **58**:71–82. doi:10.1016/j.molcel.2015.02.010
8. Azevedo C, Singh J, Steck N, Hofer A, Ruiz FA, Singh T, Jessen HJ, Saiardi A. 2018. Screening a Protein Array with Synthetic Biotinylated Inorganic Polyphosphate To Define the Human PolyP-ome. *ACS Chem Biol* **13**:1958–1963. doi:10.1021/acschembio.8b00357
9. Baev AY, Angelova PR, Abramov AY. 2020. Inorganic polyphosphate is produced and hydrolyzed in F0F1-ATP synthase of mammalian mitochondria. *Biochem J* **477**:1515–1524. doi:10.1042/BCJ20200042
10. Beaufay F, Amemiya HM, Guan J, Basalla J, Meinen BA, Chen Z, Mitra R, Bardwell JCA, Biteen JS, Vecchiarelli AG, Freddolino PL, Jakob U. 2021. Polyphosphate drives bacterial heterochromatin formation. *Sci Adv* **7**:eabk0233. doi:10.1126/sciadv.abk0233
11. Bolesch DG, Keasling JD. 2000. Polyphosphate binding and chain length recognition of Escherichia coli exopolyphosphatase. *J Biol Chem* **275**:33814–33819. doi:10.1074/jbc.M002039200
12. Bru S, Jiménez J, Canadell D, Ariño J, Clotet J. 2016a. Improvement of biochemical methods of polyP quantification. *Microb Cell* **4**:6–15. doi:10.15698/mic2017.01.551
13. Bru S, Martínez-Laínez JM, Hernández-Ortega S, Quandt E, Torres-Torronteras J, Martí R, Canadell D, Ariño J, Sharma S, Jiménez J, Clotet J. 2016b. Polyphosphate is involved in cell cycle progression and genomic stability in Saccharomyces cerevisiae. *Mol Microbiol* **101**:367–380. doi:10.1111/mmi.13396
14. Bru S, Samper-Martín B, Quandt E, Hernández-Ortega S, Martínez-Laínez JM, Garí E, Rafel M, Torres-Torronteras J, Martí R, Ribeiro MPC, Jiménez J, Clotet J. 2017. Polyphosphate is a key factor for cell survival after DNA damage in eukaryotic cells. *DNA Repair (Amst)* **57**:171–178.

doi:10.1016/j.dnarep.2017.08.001
15. Christ JJ, Willbold S, Blank LM. 2020. Methods for the analysis of polyphosphate in the life sciences. *Anal Chem* **92**:4167–4176. doi:10.1021/acs.analchem.9b05144
16. Cremers CM, Knoefler D, Gates S, Martin N, Dahl J-U, Lempart J, Xie L, Chapman MR, Galvan V, Southworth DR, Jakob U. 2016. Polyphosphate: A conserved modifier of amyloidogenic processes. *Mol Cell* **63**:768–780. doi:10.1016/j.molcel.2016.07.016
17. Desfougères Y, Saiardi A, Azevedo C. 2020. Inorganic polyphosphate in mammals: where's Wally? *Biochem Soc Trans* **48**:95–101. doi:10.1042/BST20190328
18. Dunn T, Gable K, Beeler T. 1994. Regulation of cellular Ca2+ by yeast vacuoles. *J Biol Chem* **269**:7273–7278. doi:10.1016/S0021-9258(17)37279-4
19. Fernandes-Cunha GM, McKinlay CJ, Vargas JR, Jessen HJ, Waymouth RM, Wender PA. 2018. Delivery of Inorganic Polyphosphate into Cells Using Amphipathic Oligocarbonate Transporters. *ACS Cent Sci* **4**:1394–1402. doi:10.1021/acscentsci.8b00470
20. Ghosh S, Shukla D, Suman K, Lakshmi BJ, Manorama R, Kumar S, Bhandari R. 2013. Inositol hexakisphosphate kinase 1 maintains hemostasis in mice by regulating platelet polyphosphate levels. *Blood* **122**:1478–1486. doi:10.1182/blood-2013-01-481549
21. Grigorian M, Mandal L, Hartenstein V. 2011. Hematopoiesis at the onset of metamorphosis: terminal differentiation and dissociation of the Drosophila lymph gland. *Dev Genes Evol* **221**:121–131. doi:10.1007/s00427-011-0364-6
22. Handke B, Poernbacher I, Goetze S, Ahrens CH, Omasits U, Marty F, Simigdala N, Meyer I, Wollscheid B, Brunner E, Hafen E, Lehner CF. 2013. The hemolymph proteome of fed and starved Drosophila larvae. *PLoS ONE* **8**:e67208. doi:10.1371/journal.pone.0067208
23. Hohenwallner W, Wimmer E. 1973. The Malachite green micromethod for the determination of inorganic phosphate. *Clin Chim Acta* **45**:169–175. doi:10.1016/0009-8981(73)90406-3
24. Holmström KM, Marina N, Baev AY, Wood NW, Gourine AV, Abramov AY. 2013. Signalling properties of inorganic polyphosphate in the mammalian brain. *Nat Commun* **4**:1362. doi:10.1038/ncomms2364
25. Kornberg A, Rao NN, Ault-Riché D. 1999. Inorganic polyphosphate: a molecule of many functions. *Annu Rev Biochem* **68**:89–125. doi:10.1146/annurev.biochem.68.1.89
26. Kornberg A. 1995. Inorganic polyphosphate: toward making a forgotten polymer unforgettable. *J Bacteriol* **177**:491–496. doi:10.1128/jb.177.3.491-496.1995
27. Kulakova AN, Hobbs D, Smithen M, Pavlov E, Gilbert JA, Quinn JP, McGrath JW. 2011. Direct quantification of inorganic polyphosphate in microbial cells using 4'-6-diamidino-2-phenylindole (DAPI). *Environ Sci Technol* **45**:7799–7803. doi:10.1021/es201123r
28. Montilla M, Hernández-Ruiz L, García-Cozar FJ, Alvarez-Laderas I, Rodríguez-Martorell J, Ruiz FA. 2012. Polyphosphate binds to human von Willebrand factor in vivo and modulates its interaction with glycoprotein Ib. *J Thromb Haemost* **10**:2315–2323. doi:10.1111/jth.12004
29. Morrissey JH, Smith SA. 2015. Polyphosphate as modulator of hemostasis, thrombosis, and inflammation. *J Thromb Haemost* **13 Suppl 1**:S92-7. doi:10.1111/jth.12896
30. Müller F, Mutch NJ, Schenk WA, Smith SA, Esterl L, Spronk HM, Schmidbauer S, Gahl WA, Morrissey JH, Renné T. 2009. Platelet polyphosphates are proinflammatory and procoagulant mediators in vivo. *Cell* **139**:1143–1156. doi:10.1016/j.cell.2009.11.001
31. Nakamura A, Kawano N, Motomura K, Kuroda A, Sekiguchi K, Miyado M, Kang W, Miyamoto Y, Hanai M, Iwai M, Yamada M, Hamatani T, Saito T, Saito H, Tanaka M, Umezawa A, Miyado

K. 2018. Degradation of phosphate polymer polyP enhances lactic fermentation in mice. *Genes Cells* **23**:904–914. doi:10.1111/gtc.12639
32. Omelon S, Georgiou J, Habraken W. 2016. A cautionary (spectral) tail: red-shifted fluorescence by DAPI-DAPI interactions. *Biochem Soc Trans* **44**:46–49. doi:10.1042/BST20150231
33. Omelon S, Georgiou J, Henneman ZJ, Wise LM, Sukhu B, Hunt T, Wynnyckyj C, Holmyard D, Bielecki R, Grynpas MD. 2009. Control of vertebrate skeletal mineralization by polyphosphates. *PLoS ONE* **4**:e5634. doi:10.1371/journal.pone.0005634
34. Petitou M, Tuy F, Rosenfeld C. 1978. A simplified procedure for organic phosphorus determination from phospholipids. *Anal Biochem* **91**:350–353. doi:10.1016/0003-2697(78)90849-7
35. Pick U, Weiss M. 1991. Polyphosphate Hydrolysis within Acidic Vacuoles in Response to Amine-Induced Alkaline Stress in the Halotolerant Alga Dunaliella salina. *Plant Physiol* **97**:1234–1240. doi:10.1104/pp.97.3.1234
36. Puy C, Tucker EI, Ivanov IS, Gailani D, Smith SA, Morrissey JH, Gruber A, McCarty OJT. 2016. Platelet-Derived Short-Chain Polyphosphates Enhance the Inactivation of Tissue Factor Pathway Inhibitor by Activated Coagulation Factor XI. *PLoS ONE* **11**:e0165172. doi:10.1371/journal.pone.0165172
37. Rangarajan ES, Nadeau G, Li Y, Wagner J, Hung M-N, Schrag JD, Cygler M, Matte A. 2006. The structure of the exopolyphosphatase (PPX) from Escherichia coli O157:H7 suggests a binding mode for long polyphosphate chains. *J Mol Biol* **359**:1249–1260. doi:10.1016/j.jmb.2006.04.031
38. Ruiz FA, Lea CR, Oldfield E, Docampo R. 2004. Human platelet dense granules contain polyphosphate and are similar to acidocalcisomes of bacteria and unicellular eukaryotes. *J Biol Chem* **279**:44250–44257. doi:10.1074/jbc.M406261200
39. Saito K, Ohtomo R, Kuga-Uetake Y, Aono T, Saito M. 2005. Direct labeling of polyphosphate at the ultrastructural level in Saccharomyces cerevisiae by using the affinity of the polyphosphate binding domain of Escherichia coli exopolyphosphatase. *Appl Environ Microbiol* **71**:5692–5701. doi:10.1128/AEM.71.10.5692-5701.2005
40. Samper-Martín B, Sarrias A, Lázaro B, Pérez-Montero M, Rodríguez-Rodríguez R, Ribeiro MPC, Bañón A, Wolfgeher D, Jessen HJ, Alsina B, Clotet J, Kron SJ, Saiardi A, Jiménez J, Bru S. 2021. Polyphosphate degradation by Nudt3-Zn2+ mediates oxidative stress response. *Cell Rep* **37**:110004. doi:10.1016/j.celrep.2021.110004
41. Seidlmayer LK, Gomez-Garcia MR, Blatter LA, Pavlov E, Dedkova EN. 2012. Inorganic polyphosphate is a potent activator of the mitochondrial permeability transition pore in cardiac myocytes. *J Gen Physiol* **139**:321–331. doi:10.1085/jgp.201210788
42. Sinenko SA, Kim EK, Wynn R, Manfruelli P, Ando I, Wharton KA, Perrimon N, Mathey-Prevot B. 2004. Yantar, a conserved arginine-rich protein is involved in Drosophila hemocyte development. *Dev Biol* **273**:48–62. doi:10.1016/j.ydbio.2004.05.022
43. Sinenko SA, Mathey-Prevot B. 2004. Increased expression of Drosophila tetraspanin, Tsp68C, suppresses the abnormal proliferation of ytr-deficient and Ras/Raf-activated hemocytes. *Oncogene* **23**:9120–9128. doi:10.1038/sj.onc.1208156
44. Smith SA, Choi SH, Collins JNR, Travers RJ, Cooley BC, Morrissey JH. 2012. Inhibition of polyphosphate as a novel strategy for preventing thrombosis and inflammation. *Blood* **120**:5103–5110. doi:10.1182/blood-2012-07-444935
45. Smith SA, Choi SH, Davis-Harrison R, Huyck J, Boettcher J, Rienstra CM, Morrissey JH. 2010.

Polyphosphate exerts differential effects on blood clotting, depending on polymer size. *Blood* **116**:4353–4359. doi:10.1182/blood-2010-01-266791
46. Smith SA, Mutch NJ, Baskar D, Rohloff P, Docampo R, Morrissey JH. 2006. Polyphosphate modulates blood coagulation and fibrinolysis. *Proc Natl Acad Sci USA* **103**:903–908. doi:10.1073/pnas.0507195103
47. Suess PM, Smith SA, Morrissey JH. 2020. Platelet polyphosphate induces fibroblast chemotaxis and myofibroblast differentiation. *J Thromb Haemost* **18**:3043–3052. doi:10.1111/jth.15066
48. Tammenkoski M, Koivula K, Cusanelli E, Zollo M, Steegborn C, Baykov AA, Lahti R. 2008. Human metastasis regulator protein H-prune is a short-chain exopolyphosphatase. *Biochemistry* **47**:9707–9713. doi:10.1021/bi8010847
49. Tanious FA, Veal JM, Buczak H, Ratmeyer LS, Wilson WD. 1992. DAPI (4',6-diamidino-2-phenylindole) binds differently to DNA and RNA: minor-groove binding at AT sites and intercalation at AU sites. *Biochemistry* **31**:3103–3112. doi:10.1021/bi00127a010
50. Ugochukwu E, Lovering AL, Mather OC, Young TW, White SA. 2007. The crystal structure of the cytosolic exopolyphosphatase from Saccharomyces cerevisiae reveals the basis for substrate specificity. *J Mol Biol* **371**:1007–1021. doi:10.1016/j.jmb.2007.05.066
51. Van Veldhoven PP, Mannaerts GP. 1987. Inorganic and organic phosphate measurements in the nanomolar range. *Anal Biochem* **161**:45–48. doi:10.1016/0003-2697(87)90649-x
52. Vlisidou I, Wood W. 2015. Drosophila blood cells and their role in immune responses. *FEBS J* **282**:1368–1382. doi:10.1111/febs.13235
53. Wang X, Shi C, Mo J, Xu Y, Wei W, Zhao J. 2020. An inorganic biopolymer polyphosphate controls positively charged protein phase transitions. *Angew Chem Int Ed* **59**:2679–2683. doi:10.1002/anie.201913833
54. Wei ZZ, Vatcher G, Tin AHY, Teng JL, Wang J, Cui QH, Chen JG, Yu ACH. 2015. Positively-charged semi-tunnel is a structural and surface characteristic of polyphosphate-binding proteins: an in-silico study. *PLoS ONE* **10**:e0123713. doi:10.1371/journal.pone.0123713
55. Wiame JM. 1947. The metachromatic reaction of hexametaphosphate. *J Am Chem Soc* **69**:3146. doi:10.1021/ja01204a508
56. Yoo NG, Dogra S, Meinen BA, Tse E, Haefliger J, Southworth DR, Gray MJ, Dahl J-U, Jakob U. 2018. Polyphosphate Stabilizes Protein Unfolding Intermediates as Soluble Amyloid-like Oligomers. *J Mol Biol* **430**:4195–4208. doi:10.1016/j.jmb.2018.08.016
57. Zhu Y, Huang W, Lee SSK, Xu W. 2005. Crystal structure of a polyphosphate kinase and its implications for polyphosphate synthesis. *EMBO Rep* **6**:681–687. doi:10.1038/sj.embor.7400448

Figure legends:

Fig 1: Polyphosphate extraction and quantification from flies. A) Structure of linear polyphosphates, **B)** Schematic of citrate saturated phenol-chloroform based polyphosphate extraction from *Drosophila* larvae. **C)** Schematic of polyphosphate quantification using Malachite Green. **D)** Sets of 5, 10, 20 third instar larvae show increasing amounts of polyphosphate (in Pi terms), N=5. **E)** The sets used in **(D)** are plotted as polyphosphate content per larvae to show the variation of extraction. **F)** Sets of third instar larval polyphosphate normalised protein content, N=5. **G)** Table showing absolute numbers used in **(E)** and **(F)**. Statistics: Student's *t*-test with P > 0.001, error bar - S.D.

Supplementary Fig 1: Yeast exopolyphosphatase (*Sc*PPX) purification. A) 10% PAGE showing purification of *Sc*PPX protein using Ni-NTA column. **B)** 10% PAGE showing *Sc*PPX protein after Size Exclusion Chromatography. *Sc*PPX purifies at around 47 KDa between 50KDa and 37KDa bands of protein standard.

Fig 2: Polyphosphate quantification. A) Quantification of polyphosphate across embryonic stages. n=75 in each time point, N=3. **B)** Quantification of polyP across a fly life cycle - embryos (n=75), first instar larvae (n=25), second instar larvae (n=25), feeding third instar larvae (n=10), non feeding third instar larvae (n=10), prepupae (n=20), one day old pupae (n=20), pharate (adult) (n=10). N≥3. Statistics: Student's *t*-test with P > 0.001, error bar - S.D. **C)** Quantification of polyphosphate from various cellular fractions - nucleus, mitochondria, lysosome, post lysosomal pellet, cytosol extracted from 30 larvae in each set. N=7. Statistics: Student's *t*-test with P > 0.001, error bar - S.D. The tabulated values of experimental data are provided beside each figure.

Fig 3: Polyphosphate staining of *Drosophila* tissues with PPBD. A) Schematic of GST-PPBD staining to detect polyP. **B)** Staining of larval salivary glands with DAPI (nucleus; cyan) and anti-GST antibody

(GST; orange hot). **B i, iii)** Control: DAPI (nucleus; cyan) and anti-GST antibody (GST; orange hot). **B ii, iv)** DAPI (nucleus; cyan) and anti-GST antibody (GST-PPBD-Polyphosphate; orange hot). **C-D)** Salivary gland stained with DAPI (cyan), Fibrillarin (magenta) and anti-GST antibody (orange hot) to detect polyphosphate colocalization within nucleolar fractions **(C)** is stained with GST control. **(D)** is stained with GST-PPBD. **E-G)** Wing imaginal disc stained with DAPI (cyan) and anti-GST antibody (orange hot) to detect polyphosphate. **(E)** is stained with GST control. **(F)** is stained with GST-PPBD. **(G)** is zoomed in image of **(F)** to show nuclear and cytoplasmic polyphosphate staining.

Supplementary Fig 2: Polyphosphate staining of several *Drosophila* tissues with PPBD. B, D, F, H, J, L, N, P) Control: tissues are stained with DAPI (nucleus; cyan) and anti-GST antibody (GST; orange hot). **A, C, E, G, I, K, M, O)** Tissues are stained with DAPI (nucleus; cyan) and anti-GST antibody (GST-PPBD-Polyphosphate; orange hot). Grey scale represents the GST channel.

Fig 4: Polyphosphate staining of *Drosophila* ovaries. A) Control: stained with DAPI (nucleus; cyan) and anti-GST antibody (GST; orange hot). Stages covered - S1-S8. **B)** stained with DAPI (nucleus; cyan) and anti-GST antibody (GST-PPBD-Polyphosphate; orange hot). Stages covered - S1-S9. Insets reveal nucleus and part of cytoplasm across stages S4-S9 showing reducing polyphosphate signals. Yellow arrow- follicle cells, Orange arrow- nurse cells

Fig 5: Polyphosphate affects hemolymph clotting. A-B) GST-PPBD staining of plasmocytes. *Hml-Gal4>UAS GFP* reporter was used to identify plasmocytes. **A)** Control: stained with DAPI (nucleus; cyan) and anti-GST antibody (GST; orange hot). **B)** stained with DAPI (nucleus; cyan) and anti-GST antibody (GST-PPBD-Polyphosphate; orange hot). **C-D)** GST-PPBD staining of crystal cells. *Lz-Gal4>UAS mCD8::GFP* reporter was used to identify crystal cells. **C)** Control: stained with DAPI (nucleus; cyan) and anti-GST antibody (GST; orange hot). **D)** Stained with DAPI (nucleus; cyan) and anti-GST antibody (GST-PPBD-Polyphosphate; orange hot). **E-M)** Hemolymph clot fibre thickness

analysis - **E)** clot fibre thickness with water. **F)** Pi, **G)** P_{14}, **H)** P_{65} and **I)** P_{130} **. J-M)** Quantifications of **(E-I)**. N=3. Statistics: Student's *t*-test with P > 0.001, error bar - S.D. **N-V)** Hemolymph clot fibre number analysis **N)** Number of clots formed at edge of hemolymph drop incubated with water, **O)** Pi, **P)** $P_{14,}$ **Q)** P_{65}, **R)** with P_{130}. **S-V)** Quantifications of **(N-R)**. N=6. Statistics: Paired *t*-test with P > 0.001, error bar - S.D. Scale bar for **(E-I, N-R)** - 500 px, Image dimensions in pixel: 2688 x 2200

Supplementary Fig 3: Hemolymph clot fibre formation across edge of drop A) clot fibre formation upon incubation with water at T=2 minutes, **B)** T=20 minutes, **C)** clot fibres when incubated with Pi, **D)** P_{14}, **E)** P_{65}, **F)** P_{130}. Scale bar - 500 px. Image dimensions in pixel: 3513 x 2712

Fig. 1

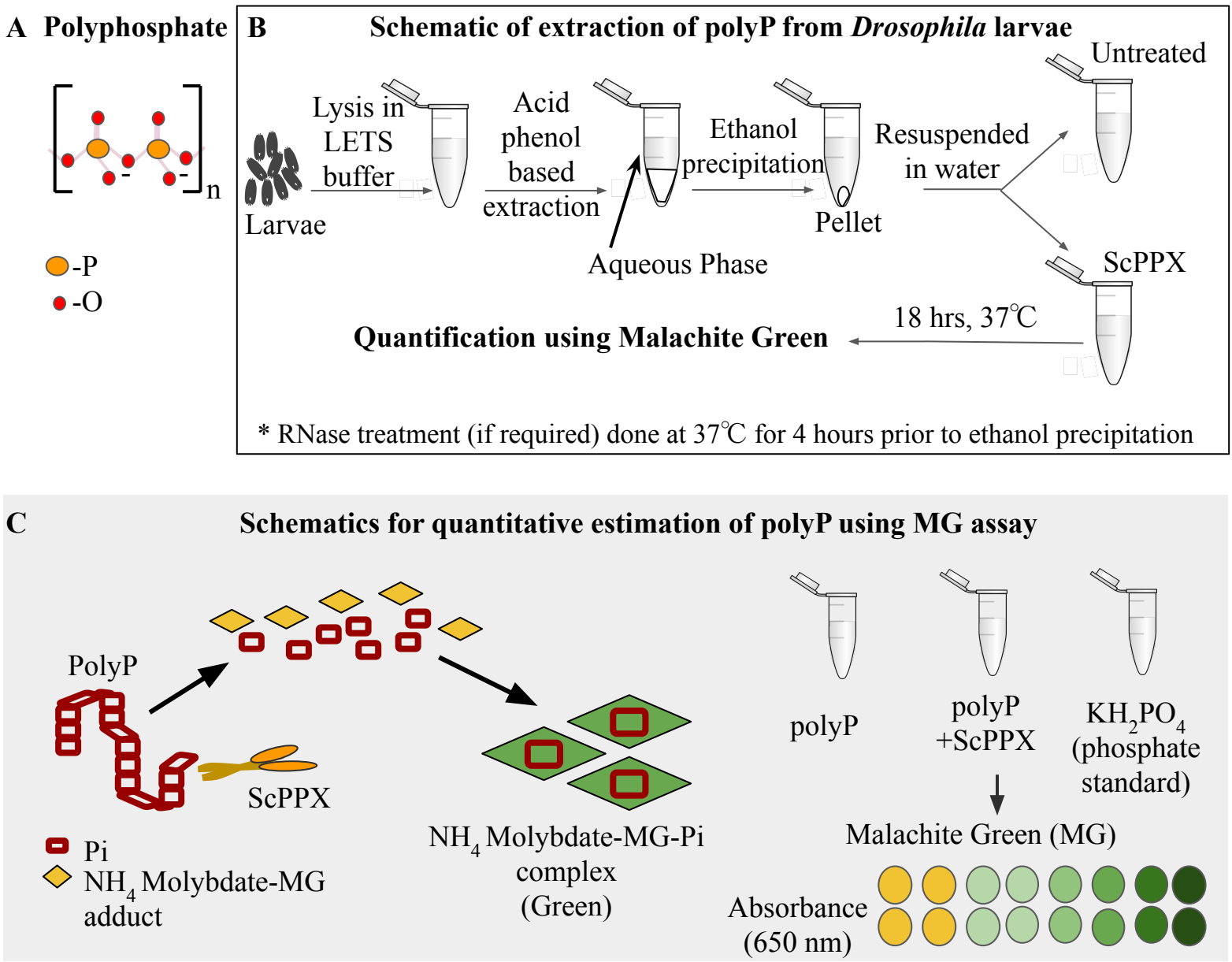

Quantitative estimation of polyP from *Drosophila* larvae

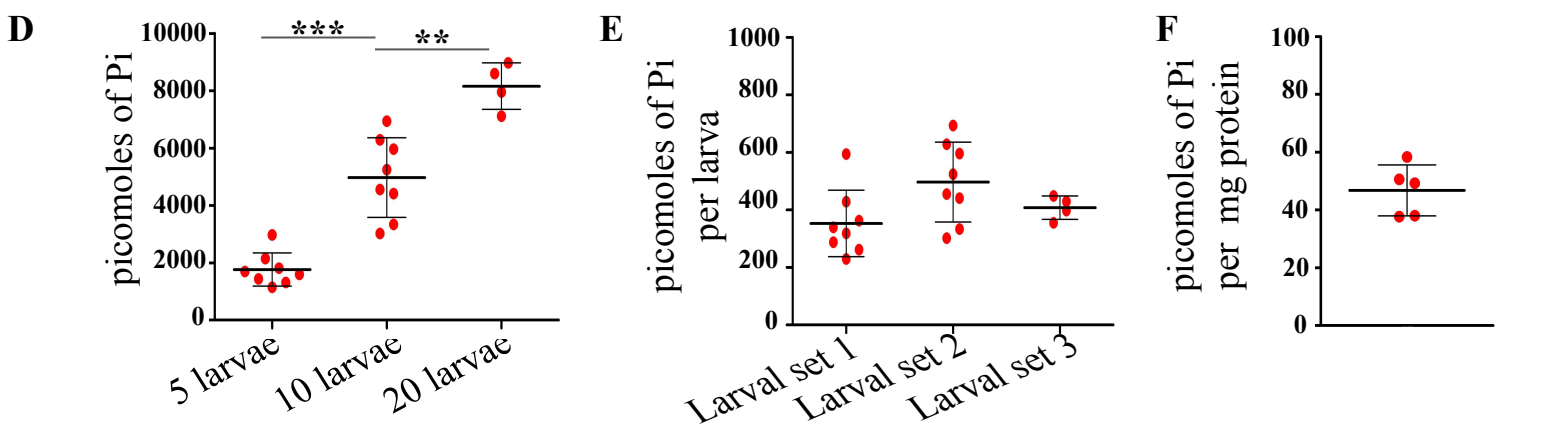

G

	PolyP quantification
Normalized to protein content	46.8 +/- 6.8 picomoles in Pi terms / mg protein
Normalised to number of larvae	565.5 +/- 326.2 picomoles in Pi terms / larva

A Estimation of polyP from various embryonic stages

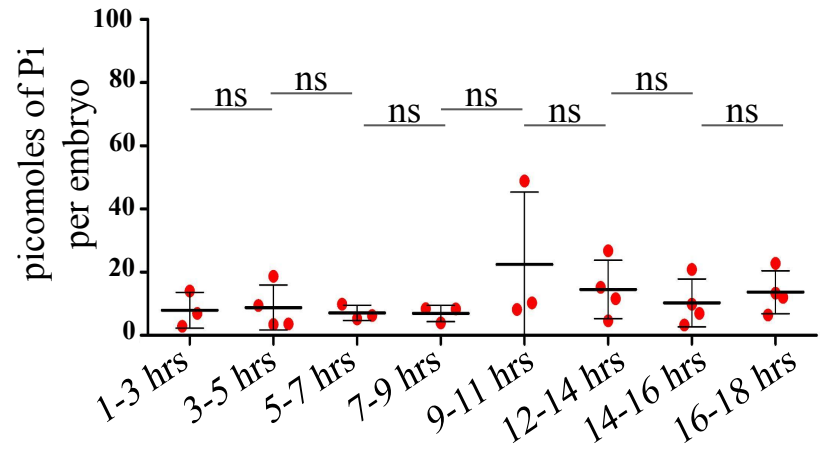

	PolyP (pmoles of Pi/ mg)
1-3 hrs	7.961 +/- 5.67
3-5 hrs	8.825 +/-7.14
5-7 hrs	7.135 +/- 2.41
7-9 hrs	6.930 +/- 2.57
9-11 hrs	22.47 +/- 22.91
12-14 hrs	14.57 +/-7.25
14-16 hrs	10.26 +/- 7.57
16-18 hrs	13.67 +/- 6.77

B Estimation of polyP from various life cycle stages

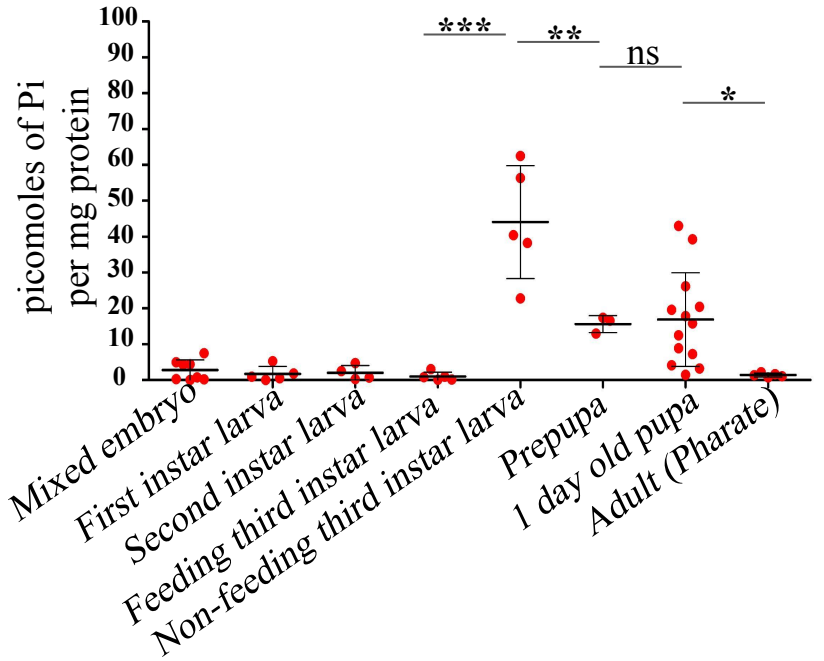

	PolyP (pmoles of Pi/mg)
Mixed embryo	2.808 +/- 2.84
First instar	1.714 +/- 2.09
Second instar	2.038 +/- 2.01
Feeding third instar	1.002 +/- 1.19
Non-feeding third instar	44.06 +/- 15.74
Prepupa	15.63 +/- 2.33
1 day old pupa	16.88 +/- 13.07
Pharate	1.398 +/- 0.56

C Estimation of polyP from various cellular fractions

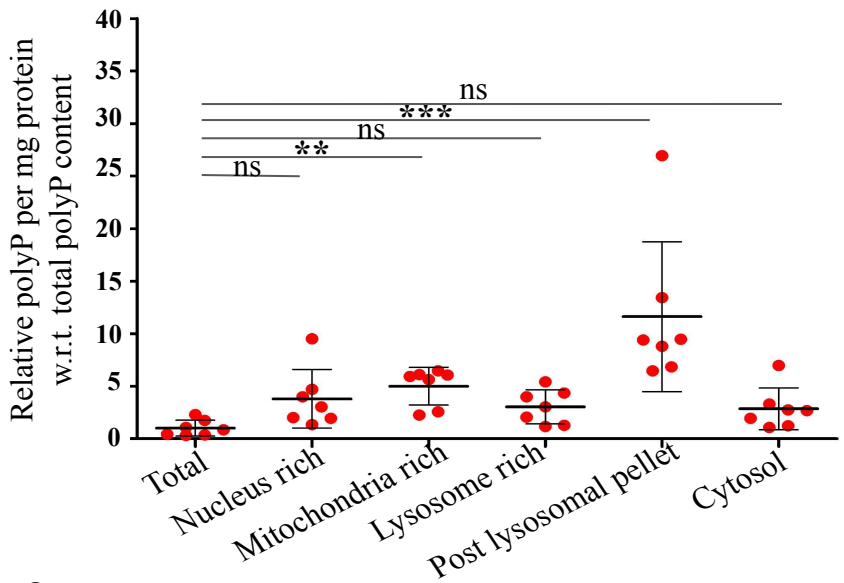

	Relative polyP level
Total	1.01 +/- 0.75
Nucleus rich	3.80 +/- 2.80
Mitochondria rich	5.00 +/- 1.78
Lysosome rich	3.05 +/- 1.63
Post lysosomal granule rich	11.62 +/- 7.13
Cytosol	2.85 +/- 1.99

Fig 2

Fig 3

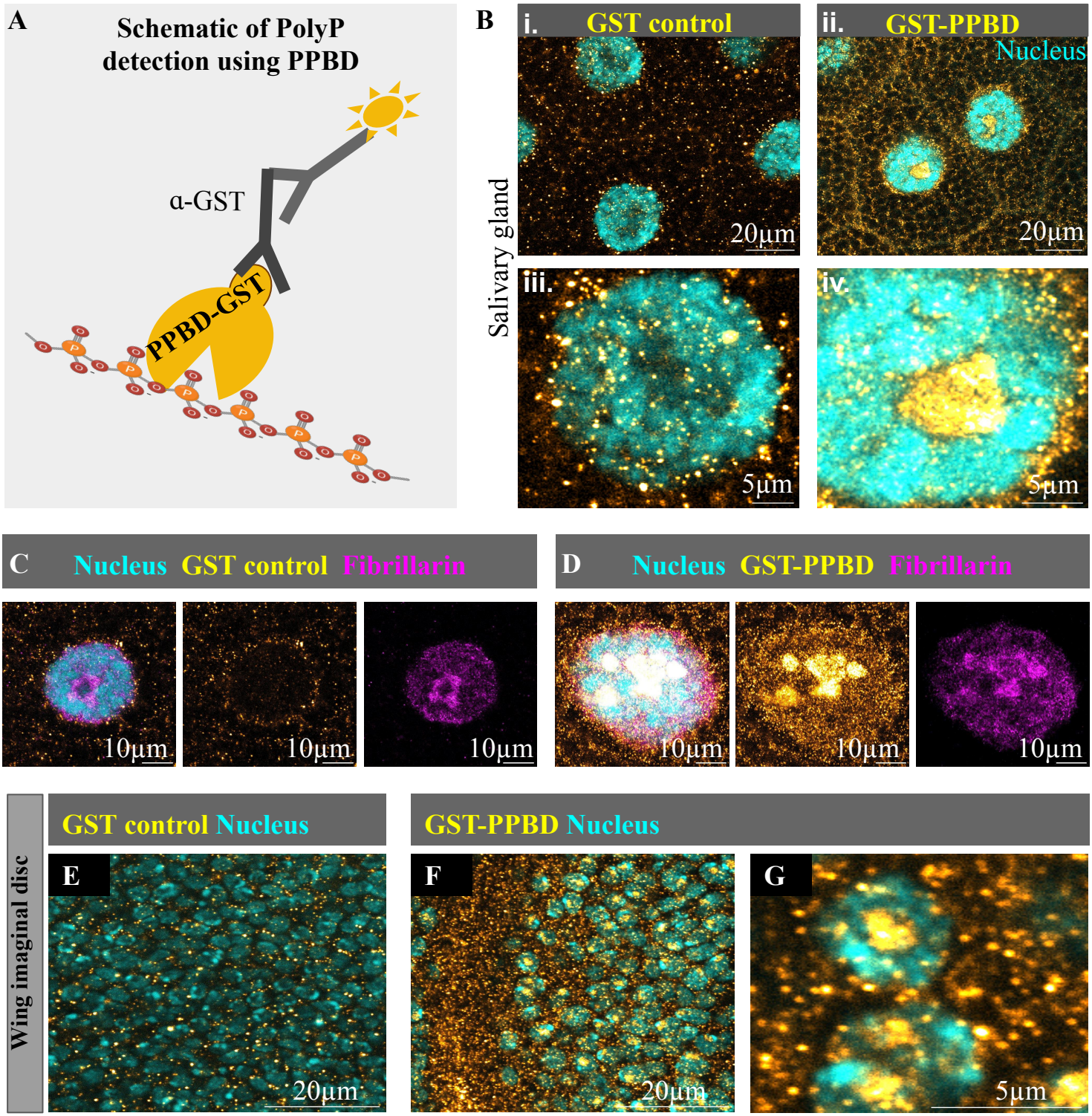
A
Schematic of PolyP detection using PPBD
α-GST
PPBD-GST
B
Salivary gland
i. GST control
ii. GST-PPBD
Nucleus
20µm
20µm
iii.
iv.
5µm
5µm
C Nucleus GST control Fibrillarin
10µm
10µm
10µm
D Nucleus GST-PPBD Fibrillarin
10µm
10µm
10µm
Wing imaginal disc
GST control Nucleus
GST-PPBD Nucleus
E
F
G
20µm
20µm
5µm

Fig 4

GST-PPBD staining of developing ovaries

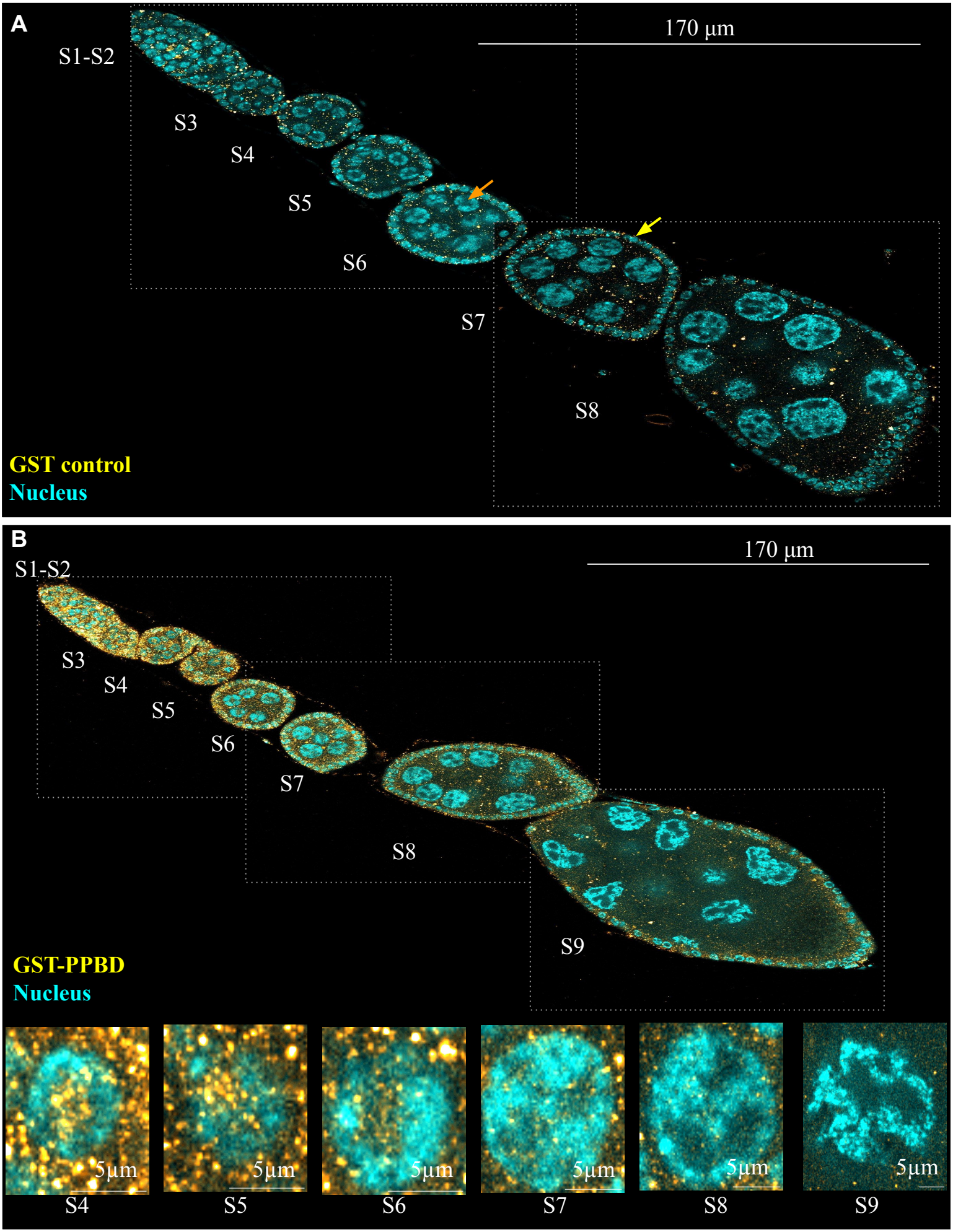

Fig 5

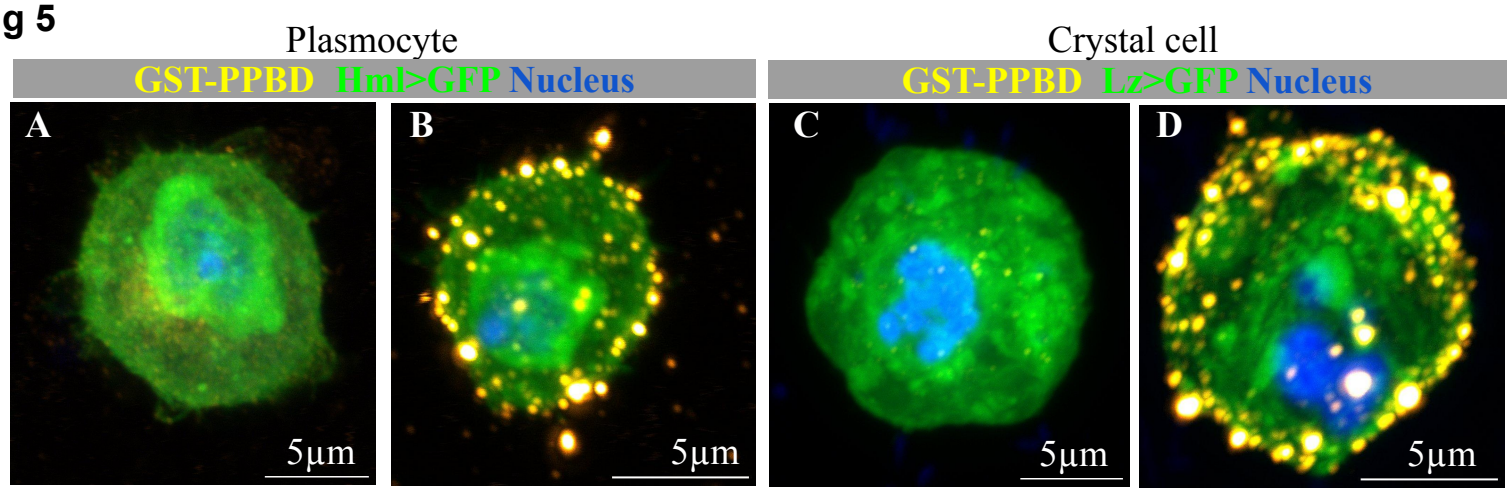

PolyP increases hemolymph clot fibre thickness

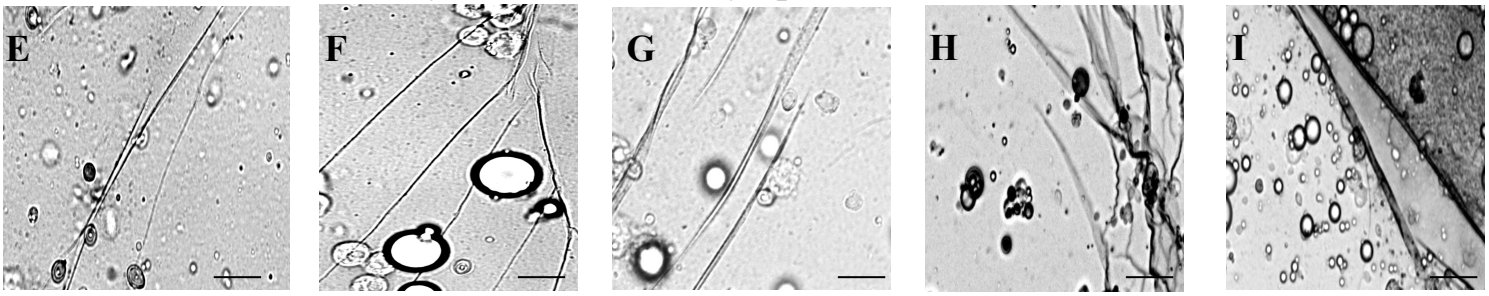

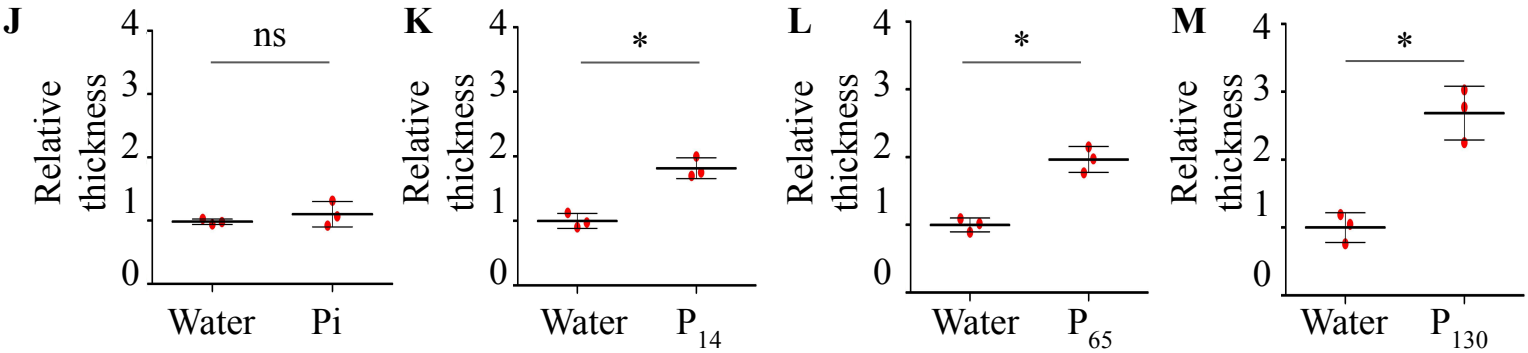

PolyP increases hemolymph clot fibre number

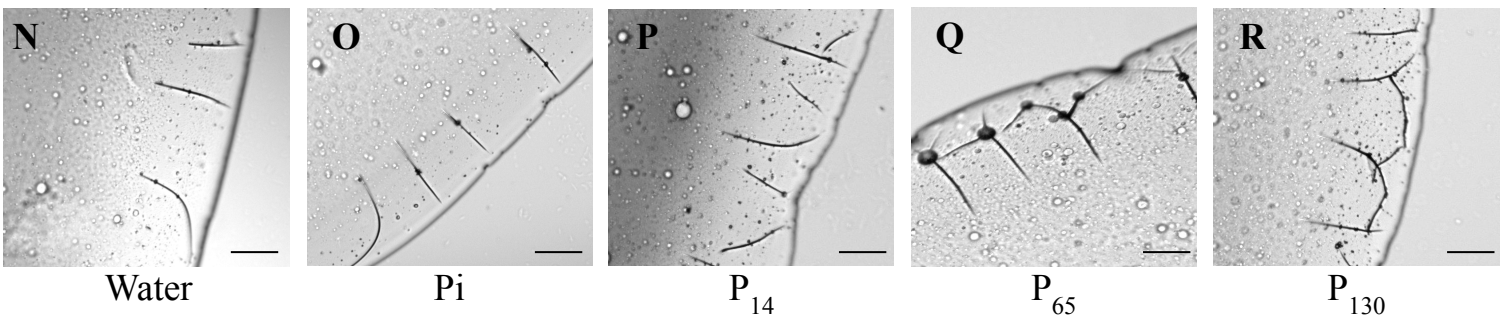

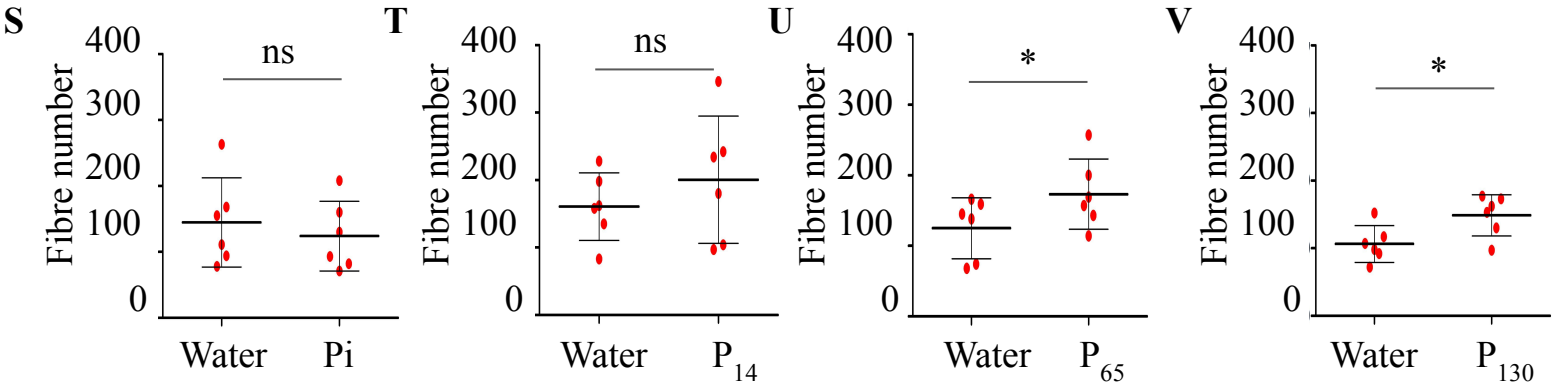

Supplementary Fig. 1

A Affinity Purification of *Sc*PPX using Ni-NTA (Step 1)

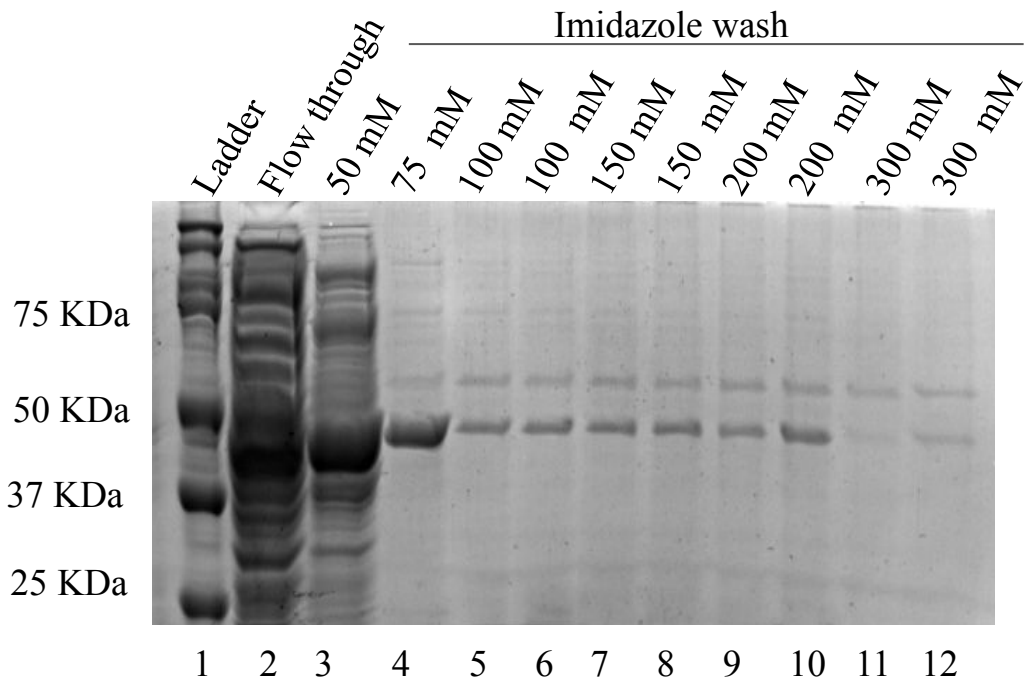

B Purification of *Sc*PPX by Size Exclusion Chromatography (Step 2)

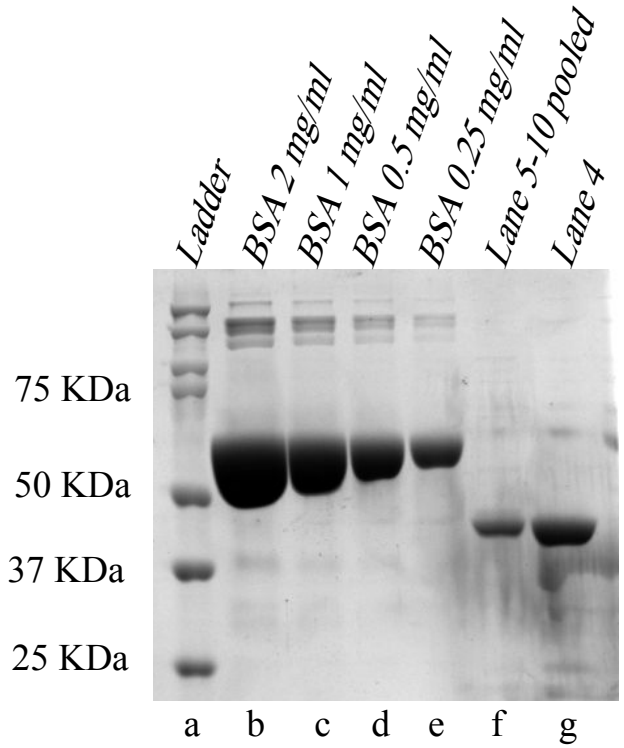

Supplementary 2 **Endogenous polyP staining in different fly tissues**

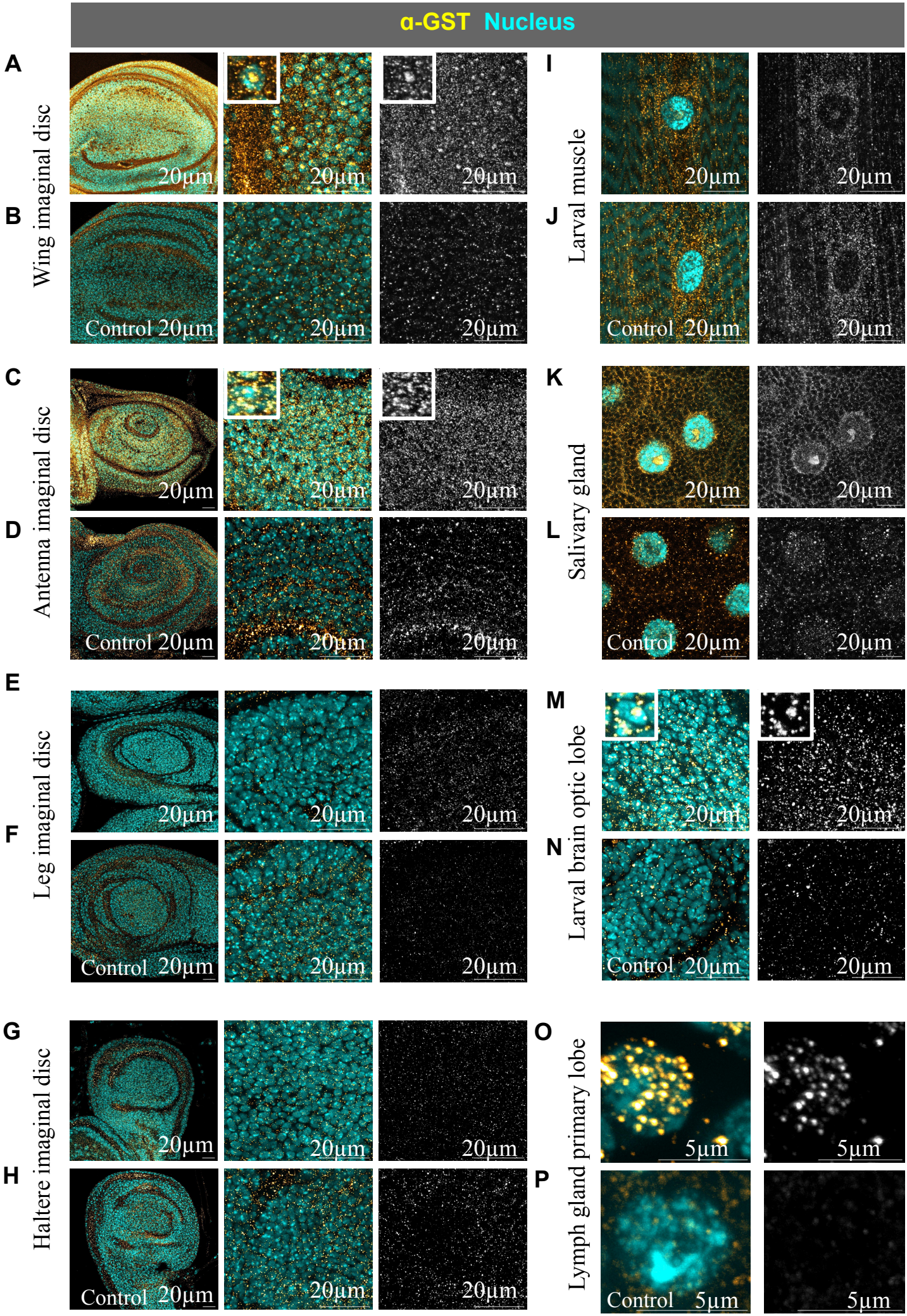

Supplementary 3
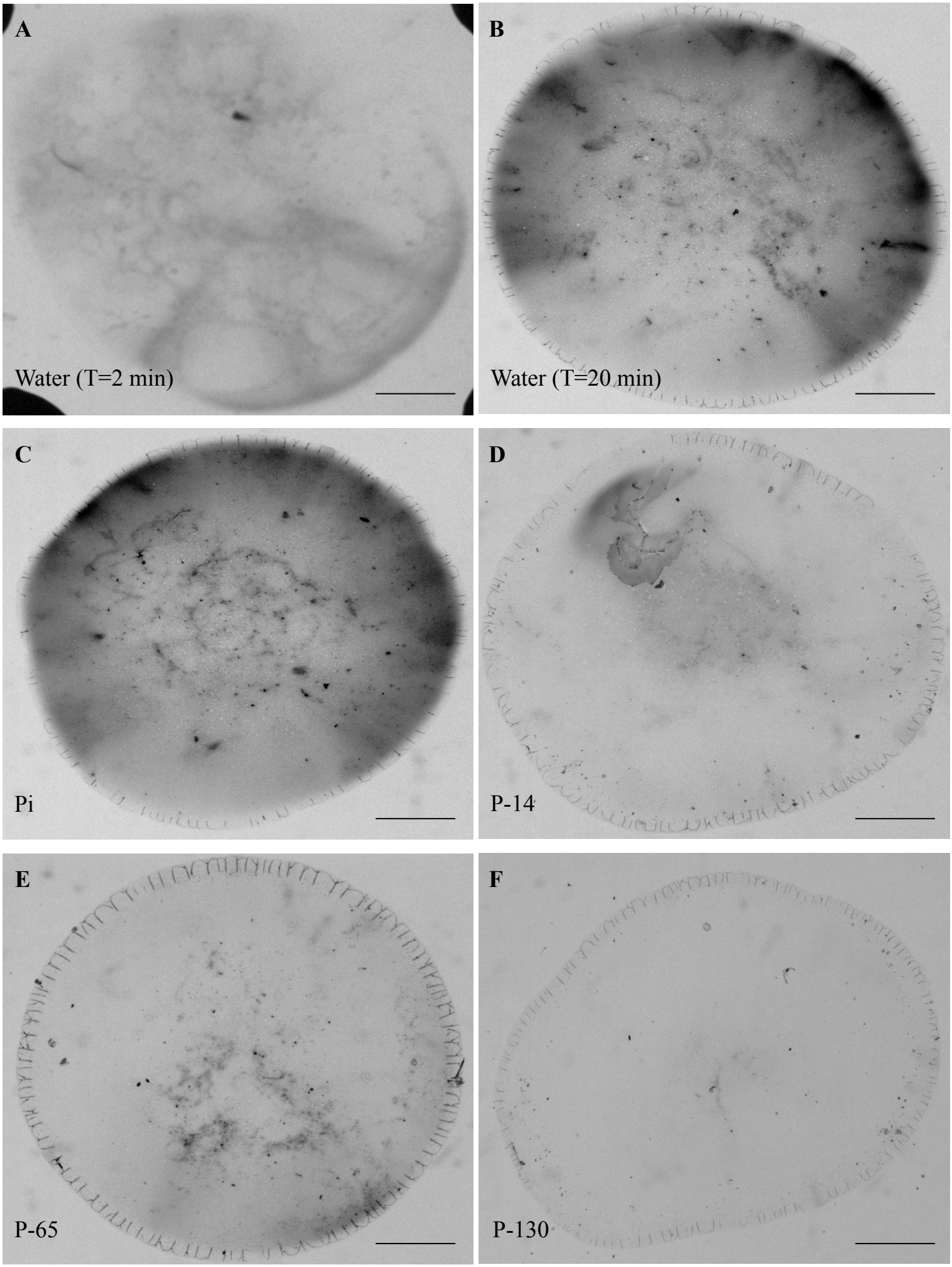
Hemolymph clot fibre formation across edge of drop after 20 minutes of incubation